Local Texture Representation for Timber Defect Recognition based on Variation of LBP

Rahillda Nadhirah Norizzaty Rahiddin[1], Ummi Raba'ah Hashim[2]
Lizawati Salahuddin[3], Kasturi Kanchymalay[4], Aji Prasetya Wibawa[5], Teo Hong Chun[6]

Fakulti Teknologi Maklumat dan Komunikasi, Universiti Teknikal Malaysia Melaka (UTeM), Melaka, Malaysia[1, 2, 3, 4]
Department of Electrical Engineering, Engineering Faculty, Universitas Negeri Malang, Malang, Indonesia[5]
Department of Information Technology and Communication, Politeknik Mersing, Johor, Malaysia[6]

Abstract—**This paper evaluates timber defect classification performance across four various Local Binary Patterns (LBP). The light and heavy timber used in the study are Rubberwood, KSK, Merbau, and Meranti, and eight natural timber defects involved; bark pocket, blue stain, borer holes, brown stain, knot, rot, split, and wane. A series of LBP feature sets were created by employing the Basic LBP, Rotation Invariant LBP, Uniform LBP, and Rotation Invariant Uniform LBP in a phase of feature extraction procedures. Several common classifiers were used to further separate the timber defect classes, which are Artificial Neural Network (ANN), J48 Decision Tree (J48), and K-Nearest Neighbor (KNN). Uniform LBP with ANN classifier provides the best performance at 63.4%, superior to all other LBP types. Features from Merbau provide the greatest F-measure when comparing the performance of the ANN classifier with Uniform LBP across timber fault classes and clean wood, surpassing other feature sets.**

Keywords—*Automated visual inspection; local binary pattern; timber defect classification; texture feature; feature extraction*

I. INTRODUCTION

Malaysia is known for its biological diversity concerning forests and marine environments, making it a megadiverse country. Since 2017, the timber sector has substantially influenced the gross domestic product (GDP). It contributed around RM 759 million to the total foreign investment. It is expected to expand by 65 per cent (RM 491.7 million), augmented by the domestic investment of around RM 267.3 million (35 per cent) annually by 2020 [1]. The amount and distribution of naturally occurring timber flaws have worried timber experts; hence, an appropriate detection method is a crucial examination procedure in the timber industry of Malaysia [2-3].

However, due to its susceptibility and the possibility of human mistakes, manual visual defect evaluation is not only acknowledged as being inaccurate in the timber industry but is also physically demanding. Acute headaches and eye fatigue are connected to strenuous labour [3–5]. The results of the detecting procedure have a significant impact on the quality of timber products [6]. Overlooked or defective products could negatively influence the industry, jeopardizing safety and causing revenue loss due to the inability to address failure or liability claims. As a result, product quality control is critical to prevent manufacturing mistakes and defects before products reach the shipping stage.

The Automated Visual Inspection (AVI) method includes automated image capture, enhancement, segmentation, feature extraction, and categorization. AVI is a completely automated extraction and categorization procedure that would enhance the inspection process and lower labour expenditures [7–9].

This research aims to classify timber faults using a pattern recognition technique contributing to AVI, emphasizing the feature extraction stage. Several studies have used Local Binary Pattern (LBP) to detect timber flaws [10]. LBP can accurately recognize and detect timber defects [11–14]. The technique was considered superior for feature extraction to other techniques based on the research [15].

LBP is still an area of active research in different domains. More recently, extended the methods using LBP to extract features from new finger vein images to improve the recognition performance system [16], spatiotemporal data fusion for producing time-series satellite images for real-world applications [17], and new blood cell classification using a hybrid learning model based on blood cell image identification [18].

Similar work has also been pursued, which utilizes the multiple feature fusion method for video emotion recognition [19]. Each keyframe belonging to real-world video sequences is processed to extract features using Uniform LBP and the scale-invariant feature identification. Conceptually similar work was performed that used LBP for extracting seven types of wheat texture features in East Azerbaijan Province to accelerate the seed supply for cultivation in seed supply centres [20].

The recent literature proposes several techniques related to LBP. Recent work used pseudo-visual search and the histogram of oriented gradients (HOG)–LBP feature fusion for intelligent vehicle detection in severe weather [21]. In addition, to completing local quartet patterns, a new version of LBP plays a crucial role in fabric textile quality-control systems [22]. Moreover, edge-aware filtering and improved LBP (EF-ALBP) is a robust edge extraction method for medical images having redundant noise, blurred details, and low contrast [23].

This study aims to recognize the general challenges concerning the automated visual inspection of timber. The focus was on the feature extraction approach and evaluating the timber defect classification performance across LBP variants. Firstly, we focused on constructing rotation-invariant uniform

feature representation of timber defects based on statistical texture features using a variation of LBP (Rotation Invariant Uniform LBP, Rotation Invariant LBP, Uniform LBP, and Basic LBP). The timber defect images dataset, labelled and validated by industry experts [3], was used here. The dataset represented several species of Malaysian hardwood, namely Rubberwood, KSK, Meranti and Merbau. Sixteen feature sets were produced and tested in the next phase. Subsequently, we evaluated timber defect class discrimination based on sixteen proposed texture feature sets using classification accuracy measures. The performance of the suggested feature set was confirmed by evaluating classification accuracy metrics with the help of common classifiers (ANN, KNN, and J48).

Finally, we compared the performance of the proposed feature sets across timber defects. Due to the superior performance of the ANN classifier in earlier studies compared to other classifiers, we chose to use it. We also used Uniform LBP because of its high classification accuracy than other LBP types. Extensive analysis revealed that all timber species displayed respectable classification accuracy, demonstrating the value of the suggested criteria in class distinction. The discriminating performance of the suggested feature sets across all classes highlighted the possibility of defect detection applications for future research, even though the study focused on identifying defects over clean wood.

II. MATERIALS AND METHODS

A. Approach Overview

This study used the timber defect dataset from the UTeM database [3]. Nine different types of timber defects, including clear wood as shown in Table I, were extracted from 3600 timber defect images (900 samples for each timber species, 100 samples for each timber defect) on several timber species. The dataset for timber defects includes 630 training pictures of clean wood and eight types of natural timber defects. Specimens of light timber, such as Rubberwood, while Meranti, KSK, and Merbau from heavy timbers are from several secondary timber product industries in Melaka, Malaysia, were used to augment the timber defect dataset. Sample collection was limited by the availability of the timber species based on end-products manufactured by the factories commonly used by different timber industries in Malaysia [3].

Ungraded, dressed, dried, and dirt-free sawn timbers used in rough milling were considered for this study. The collected timber samples had a 45-70 mm width, 100-150 mm length, and 18-22 mm thickness. The eight natural timber defects are wane, split, rot, knot, brown stain, borer holes, blue stain and bark pocket. Table II depicts the details of the timber defect image settings used for this research.

Fig. 1 illustrates extracting the statistical texture features based on LBP variants. First, timber defect images were converted to greyscale (tone-independent). Then, (1) is used for parameter setting: radius and the sampling point. All steps are to derive the rotation-invariant uniform formulation based on LBP variations. The LBP was performed by applying pixel labelling using an LBP thresholding formulation. The formulation uses a single parameter setting; sampling point, sp=8 and radius, R=1. Then, extracting statistical texture

features from an LBP variation for the four timber species. In phase one, sixteen feature sets have been produced and calculated using (1) to (9).

B. Feature Extraction

1) Basic local binary pattern: basic lbp produces 256 values. The LBP code for each basic LBP pixel must be determined. The pixel is labelled using decimal numbers by encoding the local structure around each pixel. For example, by deducting the value of the centre pixel, each pixel in a 3×3 neighbourhood is compared to its eight neighbours; if the result is positive, value 1 is used. In contrast, negative results generate 0. The process outputs 8-bit integers by arranging each bit clockwise, starting from the top-left to obtain eight different binary patterns. The mathematical expression of the LBP is specified in (1).

$$LBP_{P,R}(x_c, y_c) = \sum_{i=0}^{P-1} s(g_i - g_c)2^i \qquad (1)$$

TABLE I. TIMBER DEFECT CLASSES [3]

Knot	Split
Blue Stain	Brown Stain
Bark Pocket	Borer holes
Rot	Wane

TABLE II. TIMBER DEFECT IMAGE SETTINGS [3]

Sensor used	Optical sensor
Optical imaging device	Area scan cameras
Image setting	1024 by 768 pixels (300dpi) 24-bit depth and 256 intensity levels for the red, green and blue channel
Sub-image setting	60 x 60 pixels

Convert images
• Convert 3600 wood defect images to greyscale images

Parameter Setting
• radius, *R*=1
• sampling point, *sp*=8

Extract Statistical Features
• 16 statistical feature sets
  • Basic LBP - 256 features
  • Rotation Invariant LBP - 36 features
  • Uniform LBP - 59 features
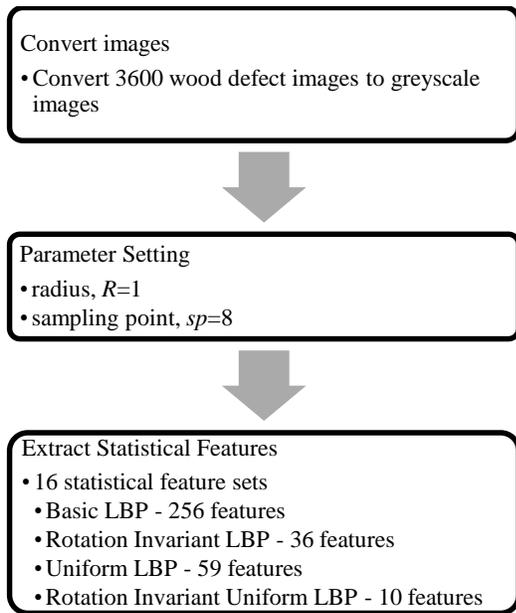 • Rotation Invariant Uniform LBP - 10 features

Fig. 1.   Process of Extracting Statistical Texture Features based on LBP Variants.

The notation (P, R) designates P sampling points on a circle of radius R; (x_c, y_c) designates the centre of a pixel, g_c represents the grey value of the centre pixel; and g_i (i=0,1,…,P-1) designates the grey value of the P sampling points next to it. Signed differences $g_i - g_c$ are interpreted as P-bit binary numbers, producing 2^i distinct values. The thresholding function s(x) is defined in (2):

$$s(x) = \begin{cases} 1 \ if \ x \geq 0 \\ 0 \ if \ x < 0 \end{cases} \tag{2}$$

2) Rotation invariant local binary pattern: Rotation invariant LBP is used to analyze and compute the value of the rotated picture [24]. The g_i grey values along the perimeter of the circle around g_c vary when the image is rotated. The binary pattern rotates in a clockwise direction, resulting in various LBP values. As a result, the lowest value of the binary pattern generated from the direction of maximal rotation is chosen for computation. Similarly, for cluster-like patterns, the rotation invariant LBP with the lowest value of the circular bitwise clockwise direction of the x bit sequence by i steps or the $ROR(x, i)$ can thus be recognize as:

$$LBP_{P,R}^{ri} = \min\{ROR(LBP_{P,R}, i) \mid i = 0,1, …, P - 1\} \tag{3}$$

Rotation invariant LBP can generate 36 different patterns.

3) Uniform local binary pattern: Since circular rotation bit patterns with 0-1 or 1-0 transitions are used to determine the LBP uniformity [25], uniformity can be identified from the two transitions comprising a single binary pattern. On the other hand, if the transitions exceed this count, i.e., if the binary pattern comprises more than two transitions, it does not belong to the uniform LBP category. Uniform LBP can be seen in patterns 00000000_2 (0 transition) and 00001000_2 (2

transitions) and each uniform pattern has a separate output label. Transition count calculation can be obtained using (4):

$$U(LBP_{P,R}) = \mid s(g_{P-1} - g_c) - s(g_0 - g_c) \mid + \sum_{i=1}^{P-1} \mid s(g_i - g_c) - s(g_{i-1} - g_c) \mid \tag{4}$$

There are $P(P - 1) + 3$ different P-bit output labels; eight sampling points produce 59 labels, where 58 are uniform and 1 is non-uniform.

4) Rotation invariant uniform local binary pattern: The superscript riu^2, which donates the maximum uniform value of two, is used by the rotation-invariant uniform patterns, as stated in (5). By definition, $P + 1$ occurs in a circular symmetric neighbour set of P pixels in uniform binary patterns. The above equation determined 27 non-uniform patterns and 9 uniform patterns. The mapping of 8-bit binary numbers from LBP_8 to $LBP_8^{riu^2}$ comprises 10 unique outputs than a 256-element lookup table:

$$LBP_{P,R}^{riu^2} = \begin{cases} \sum_{i=0}^{P-1} s(g_i - g_c) \ \ if \ U(LBP_{P,R}) \leq 2 \\ \qquad P + 1 \quad otherwise, \end{cases} \tag{5}$$

C. Evaluation of Detection Performance

1) Precision, recall, f-measure, and classification accuracy: Precision and recall are conventional and appropriate assessment metrics to evaluate the performance of content-based image retrieval. Precision and recall are calculated using positive and negative system replies for every query. [26]. In this study, clear wood images accounted for a significant part of the dataset than timber defect samples. It is typical in the secondary timber industry.

Equation (6) shows precision is the ratio of actual timber defects to the total number of detected ones. Precision, sometimes referred to as positive predictive value, results from the retrieval system's true positive and false positive images. A recall is the ratio of the total number of real defects in the timber to the total number of actual defects in timber, as defined in (7). The recall is a function of the true-positive and false-negative images in the retrieval system [27]. The F-Measure in each class is a composite measure of precision and recall, as shown in (8).

$$precision, P = \frac{number \ of \ true \ defects}{number \ of \ defects \ detected}$$

$$= \frac{true \ defects}{true \ defects + false \ defects} \tag{6}$$

$$recall, R = \frac{number \ of \ true \ defects}{number \ of \ actual \ defects}$$

$$= \frac{true \ defects}{true \ defects + false \ clear \ wood} \tag{7}$$

$$F - Measure, F = 2 \ \frac{PR}{P+R} \tag{8}$$

The experiment aims to improve experiment accuracy, typically measured using classification accuracy [28]. Classification algorithms are assessed using classification accuracy [29], as defined in (9).

$$Classification\ Accuracy\ (\%) = \frac{Number\ of\ corect\ classification}{Total\ number\ of\ samples} \cdot 100\% \qquad (9)$$

III. RESULTS AND DISCUSSION

A. Classification Performance across LBP Variants

For a more in-depth understanding of the applicability of various characteristics across each LBP variation, the best classification performance is compared to other classifiers for that version. Table III shows the F-measure for each feature set. By integrating precision and recall values, the F-measure benchmark evaluates picture segmentation and classification accuracy. Comparing the ANN classifier to the KNN and J48 classifiers produces good results.

Fig. 2 shows the mean or average percentage classification accuracy of the standard classifier across all LBP variants. Basic LBP has a 48.42% classification accuracy, while Rotation Invariant LBP is 48.7% accurate. Moreover, Uniform LBP has 56.8% accuracy values, while Rotation Invariant Uniform LBP has 52% accuracy values.

B. Classification Performance across Timber Defects

The ANN classifier delivered the best classification performance, as we previously concluded. Performance assessment continues by evaluating the ANN classifier and Uniform LBP across timber defect classes and clear wood. Since Basic, Rotation Invariant, and Rotation Invariant Uniform LBP datasets previously showed low classification performance, we will now look at the classification details of a well-performed Uniform LBP dataset only.

Fig. 3 illustrates the F-measure calculation for timber defect classes. Bark pocket, split, and borer hole classes show the lowest F-measure across all classes, achieving less than 0.63 F-value. Meanwhile, the top three F-measures across timber defect classes are wane, clear wood, and rot. The attributes of the Rubberwood dataset are the most effective in classifying

rot, wane, and brown stain. In contrast, the split was best ranked for the KSK dataset.

TABLE III. CLASSIFIERS COMPARISON WITH F-MEASURE OF LBP VARIANTS

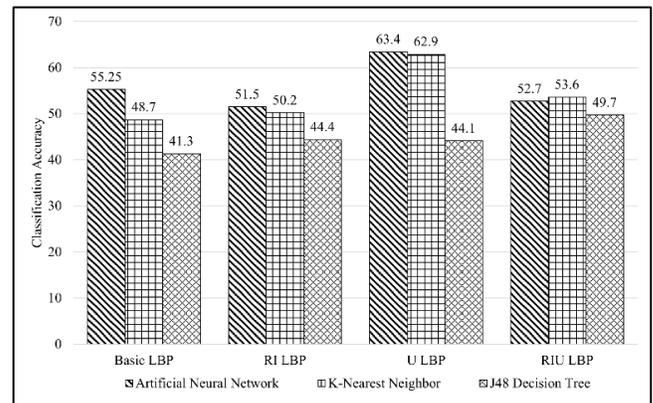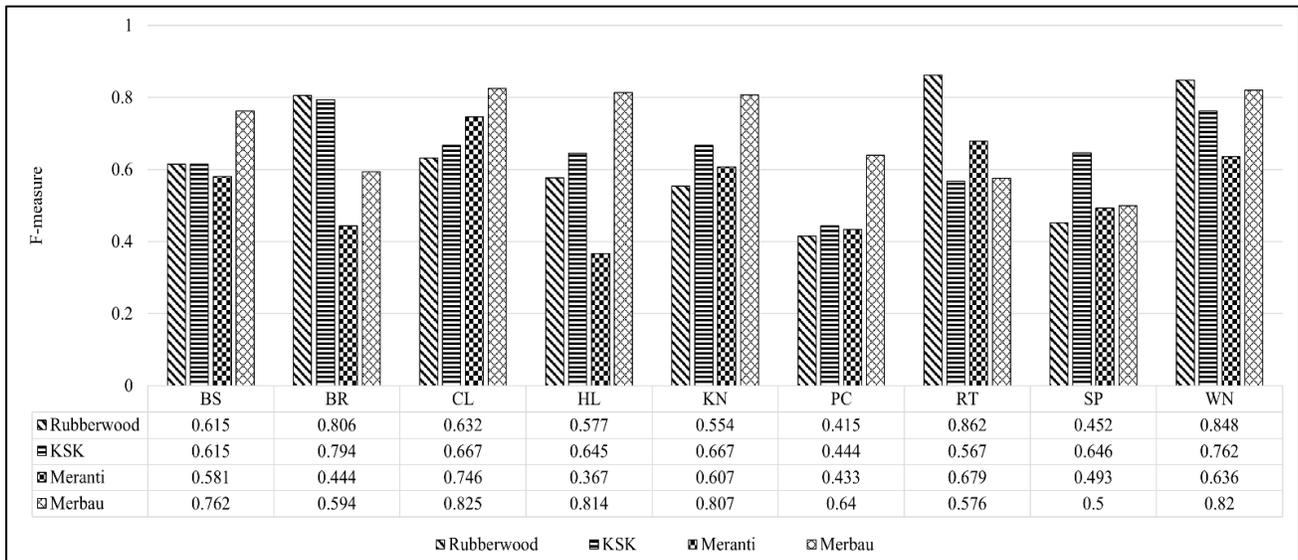| Class	F-measure	Classifier
Basic LBP	0.553	ANN
	0.487	KNN
	0.413	J48
Rotation Invariant LBP	0.515	ANN
	0.502	KNN
	0.444	J48
Uniform LBP	0.634	ANN
	0.629	KNN
	0.441	J48
Rotation Invariant Uniform LBP	0.527	ANN
	0.536	KNN
	0.497	J48

Fig. 2. The Mean or Average Percentage Classification Accuracy of the Standard Classifier Across all LBP Variants (RI LBP = Rotation Invariant LBP, U LBP = Uniform LBP, RIU LBP = Rotation Invariant Uniform LBP).

	BS	BR	CL	HL	KN	PC	RT	SP	WN
Rubberwood	0.615	0.806	0.632	0.577	0.554	0.415	0.862	0.452	0.848
KSK	0.615	0.794	0.667	0.645	0.667	0.444	0.567	0.646	0.762
Meranti	0.581	0.444	0.746	0.367	0.607	0.433	0.679	0.493	0.636
Merbau	0.762	0.594	0.825	0.814	0.807	0.64	0.576	0.5	0.82

(BS-Blue Stain, BR-Brown Stain, CL-Clear Wood, HL-Borer Holes, KN-Knot, PC-Bark Pocket, RT-Rot, SP-Split, WN-Wane)

Fig. 3. F-measure for Each Timber Defect Class, Including Clear Wood, Calculated using ANN Classifier and Uniform LBP.

Similarly, the characteristics of Merbau were the best in classifying blue stain, clear wood, borer holes, knot, and bark pocket. Merbau features provide the best F-measure when considering generalised differences among timber defect classes, beating other feature sets.

IV. CONCLUSION

The paper presented the evaluation of timber defect classification performance across LBP variants. The experiment highlights the average percentage classification accuracy for all LBP variants. Comparing all LBP types, uniform LBP with ANN classifier offers the greatest performance at 63.4%. By analyzing the performance of the ANN classifier with Uniform LBP across timber defect classes and clear wood, features from Merbau species give the best F-measure, outperforming other feature sets from other timber species. In line with the findings of this paper, it demonstrates that Merbau-derived traits were most effective for classifying blue stains, clear wood, borer holes, knots, and bark pockets. Moreover, brown stain, split, wane and rot show the lowest F-measure. In this research, statistical texture based on variations of LBP to represent wood surface characteristics was employed. Other texture feature extraction techniques could be explored to further improve the feature representation and for better discrimination capabilities between wood defects and *clear wood*. Other researchers working on certain timber defect classes focusing on applications will find this discovery useful.

ACKNOWLEDGMENT

REFERENCES

[1] MIDA, "Wood-Based and Furniture," Malaysian Investment Development Authority Official Website, 2021. https://www.mida.gov.my/industries/manufacturing/wood-based-and-furniture/.

[2] I. Cetiner, A. A. Var, and H. Cetiner, "Classification of Knot Defect Types Using Wavelets and KNN," Elektron. ir Elektrotechnika, vol. 22, no. 6, pp. 67–72, 2016, doi: 10.5755/j01.eie.22.6.17227.

[3] U. R. Hashim, S. Z. Hashim, and A. K. Muda, "Image Collection for Non-Segmenting Approach of Timber Surface Defect Detection," Int. J. Adv. Soft Comput. its Appl., vol. 7, no. 1, pp. 15–34, 2015.

[4] R. Qayyum, K. Kamal, T. Zafar, and S. Mathavan, "Wood Defects Classification Using GLCM Based Features And PSO Trained Neural Network," 2016 22nd Int. Conf. Autom. Comput. ICAC 2016 Tackling New Challenges Autom. Comput., pp. 273–277, 2016, doi: 10.1109/IConAC.2016.7604931.

[5] U. R. Hashim, S. Z. Hashim, and A. K. Muda, "Automated vision inspection of timber surface defect: A review," J. Teknol., vol. 77, no. 20, pp. 127–135, 2015, doi: 10.11113/jt.v77.6562.

[6] Y. Zhang, C. Xu, C. Li, H. Yu, and J. Cao, "Wood defect detection method with PCA feature fusion and compressed sensing," J. For. Res., vol. 26, no. 3, pp. 745–751, 2015, doi: 10.1007/s11676-015-0066-4.

[7] N. D. Abdullah, U. R. Hashim, S. Ahmad, and L. Salahuddin, "Analysis of Texture Features for Wood Defect Classification," Bull. Electr. Eng. Informatics, vol. 9, no. 1, pp. 121–128, 2020, doi: 10.11591/eei.v9i1.1553.

[8] T. H. Chun et al., "Identification of Wood Defect Using Pattern Recognition Technique," Int. J. Adv. Intell. Informatics, vol. 7, no. 2, pp. 163–176, 2021, doi: 10.26555/ijain.v7i2.588.

[9] Y. Zhang, S. Liu, W. Tu, H. Yu, and C. Li, "Using computer vision and compressed sensing for wood plate surface detection," Opt. Eng., vol. 54, no. 10, pp. 103102-1-103102–10, 2015, doi: 10.1117/1.OE.54.10.103102.

[10] T. Ojala, M. Pietikäinen, and D. Harwood, "Performance evaluation of texture measures with classification based on Kullback discrimination of distributions," Proc. - Int. Conf. Pattern Recognit., vol. 3, pp. 582–585, 1994, doi: 10.1109/ICPR.1994.576366.

[11] I. M. Khairuddin et al., "Automatic Classification of Wood Texture Using Local Binary Pattern & Fuzzy K-Nearest Neighbor," Adv. Mater. Res., vol. 903, pp. 315–320, 2014, doi: 10.4028/www.scientific.net/AMR.903.315.

[12] M. Nasirzadeh, A. A. Khazael, and M. Khalid, "Woods Recognition System Based on Local Binary Pattern," Second Int. Conf. Comput. Intell. Commun. Syst. Networks, no. 2, pp. 2–7, 2010, doi: 10.1109/CICSyN.2010.27.

[13] Z. Y. Xiang, Z. Y. Qin, L. Ying, J. L. Quan, and C. Z. Wei, "Identification of Wood Defects Based on LBP Features," in Chinese Control Conference, CCC, 2016, pp. 4202–4205, doi: 10.1109/ChiCC.2016.7554010.

[14] E. A. B. Ibrahim et al., "Evaluation of Texture Feature based on Basic Local Binary Pattern for Wood Defect Classification," Int. J. Adv. Intell. Informatics, vol. 7, no. 1, pp. 26–36, 2021, doi: 10.26555/ijain.v7i1.393.

[15] Prasetiyo, M. Khalid, R. Yusof, and F. Meriaudeau, "A Comparative Study of Feature Extraction Methods for Wood Texture Classification," 2010 Sixth Int. Conf. Signal-Image Technol. Internet Based Syst., pp. 23–29, 2010, doi: 10.1109/SITIS.2010.15.

[16] H. Ren, L. Sun, J. Guo, C. Han, and Y. Cao, "A high compatibility finger vein image quality assessment system based on deep learning," Expert Syst. Appl., vol. 196, no. January, p. 116603, 2022, doi: 10.1016/j.eswa.2022.116603.

[17] X. Zhu et al., "A novel framework to assess all-round performances of spatiotemporal fusion models," Remote Sens. Environ., vol. 274, no. March, p. 113002, 2022, doi: 10.1016/j.rse.2022.113002.

[18] K. A. Davamani, C. R. R. Robin, D. D. Robin, and L. J. Anbarasi, "Adaptive blood cell segmentation and hybrid Learning-based blood cell classification: A Meta-heuristic-based model," Biomed. Signal Process. Control, vol. 75, no. October 2021, p. 103570, 2022, doi: 10.1016/j.bspc.2022.103570.

[19] N. Samadiani et al., "A Multiple Feature Fusion Framework for Video Emotion Recognition in the Wild," Concurr. Comput. Pract. Exp., vol. 34, no. 8, pp. 1–13, 2020, doi: 10.1002/cpe.5764.

[20] M. Khojastehnazhand and M. Roostaei, "Classification of seven Iranian wheat varieties using texture features," Expert Syst. Appl., vol. 199, no. May 2021, p. 117014, 2022, doi: 10.1016/j.eswa.2022.117014.

[21] Z. Wang, J. Zhan, C. Duan, X. Guan, and K. Yang, "Vehicle Detection in Severe Weather based on Pseudo-visual Search and HOG–LBP Feature Fusion," J. Automob. Eng., vol. 236, no. 7, pp. 1607–1618, 2021, doi: 10.1177/09544070211036311.

[22] Z. Pourkaramdel, S. Fekri-Ershad, and L. Nanni, "Fabric defect detection based on completed local quartet patterns and majority decision algorithm," Expert Syst. Appl., vol. 198, no. March, p. 116827, 2022, doi: 10.1016/j.eswa.2022.116827.

[23] S. Qiao et al., "Edge Extraction Method for Medical Images based on Improved Local Binary Pattern Combined with Edge-aware Filtering," Biomed. Signal Process. Control, vol. 74, no. December 2021, p. 103490, 2022, doi: 10.1016/j.bspc.2022.103490.

[24] M. Pietikäinen, T. Ojala, and Z. Xu, "Rotation-invariant texture classification using feature distributions," Pattern Recognit., vol. 33, no. 1, pp. 43–52, 2000, doi: 10.1016/S0031-3203(99)00032-1.

[25] T. Ojala, M. Pietikäinen, and T. Mäenpää, "Multiresolution gray-scale and rotation invariant texture classification with local binary patterns," IEEE Trans. Pattern Anal. Mach. Intell., vol. 24, no. 7, pp. 971–987, 2002, doi: 10.1109/TPAMI.2002.1017623.

[26] M. Verma and B. Raman, "Local neighborhood difference pattern : A new feature descriptor for natural and texture image retrieval," Multimed. Tools Appl., no. May, 2017, doi: 10.1007/s11042-017-4834-3.

[27] P. Banerjee, A. K. Bhunia, A. Bhattacharyya, P. P. Roy, and S. Murala, "Local Neighborhood Intensity Pattern–A new texture feature descriptor

for image retrieval," Expert Syst. Appl., vol. 113, pp. 100–115, 2018, doi: 10.1016/j.eswa.2018.06.044.

[28] T. Pahlberg, M. Thurley, D. Popovic, and O. Hagman, "Crack detection in oak flooring lamellae using ultrasound-excited thermography," Infrared Phys. Technol., vol. 88, pp. 57–69, 2017, doi: 10.1016/j.infrared.2017.11.007.

[29] V. N. T. Le, B. Apopei, and K. Alameh, "Effective plant discrimination based on the combination of Local Binary Pattern operators and multiclass Support Vector Machine methods," Inf. Process. Agric., vol. 6, no. 1, pp. 116–131, 2019, doi: 10.1016/j.inpa.2018.08.002.